Supplement of Atmos. Chem. Phys., 26, 10423–10454, 2026
https://doi.org/10.5194/acp-26-10423-2026-supplement

Atmospheric Chemistry and Physics
Open Access
EGU

Supplement of

Assessment of the differences in European CH_4 emission estimates from three TROPOMI products

Aurélien Sicsik-Paré et al.

Correspondence to: Aurélien Sicsik-Paré (aurelien.sicsik-pare@lsce.ipsl.fr)

Country	Prior (Tg/yr)	Posterior SRON (Tg/yr)	BLENDED (Tg/yr)	WFMD (Tg/yr)	Surface (Tg/yr)
Germany	2.74	3.02 (+10%)	3.02 (+10%)	2.25 (-18%)	3.27 (+20%)
France	2.60	2.72 (+4%)	2.69 (+3%)	1.83 (-30%)	2.23 (-14%)
Poland	2.55	2.64 (+4%)	2.47 (-3%)	1.45 (-43%)	2.42 (-5%)
Italy	2.45	2.32 (-5%)	2.22 (-9%)	1.09 (-56%)	1.13 (-54%)
United Kingdom	2.03	2.24 (+10%)	2.20 (+8%)	1.78 (-12%)	1.70 (-16%)
Romania	1.58	1.38 (-13%)	1.27 (-19%)	0.45 (-72%)	1.27 (-20%)
Spain	1.56	1.52 (-3%)	1.34 (-14%)	0.89 (-43%)	1.49 (-4%)
Finland	1.05	1.00 (-5%)	1.07 (+1%)	0.98 (-7%)	0.82 (-22%)
Sweden	0.94	0.92 (-3%)	0.96 (+1%)	0.89 (-6%)	0.78 (-17%)
Belgium	0.74	0.78 (+5%)	0.80 (+9%)	0.47 (-37%)	0.80 (+9%)
Ireland	0.74	0.79 (+7%)	0.77 (+4%)	0.67 (-9%)	0.43 (-41%)
Netherlands	0.66	0.75 (+13%)	0.77 (+17%)	0.51 (-22%)	1.27 (+92%)
Norway	0.56	0.55 (-2%)	0.57 (+1%)	0.55 (-2%)	0.48 (-14%)
Czech Republic	0.50	0.55 (+10%)	0.50 (0%)	0.30 (-40%)	0.58 (+17%)
Austria	0.46	0.51 (+11%)	0.47 (+2%)	0.35 (-24%)	0.48 (+5%)

Table S1. Prior, posterior CH_4 emissions and the relative increments per country, for the 15 highest emitting countries and the four inversions performed in this study.

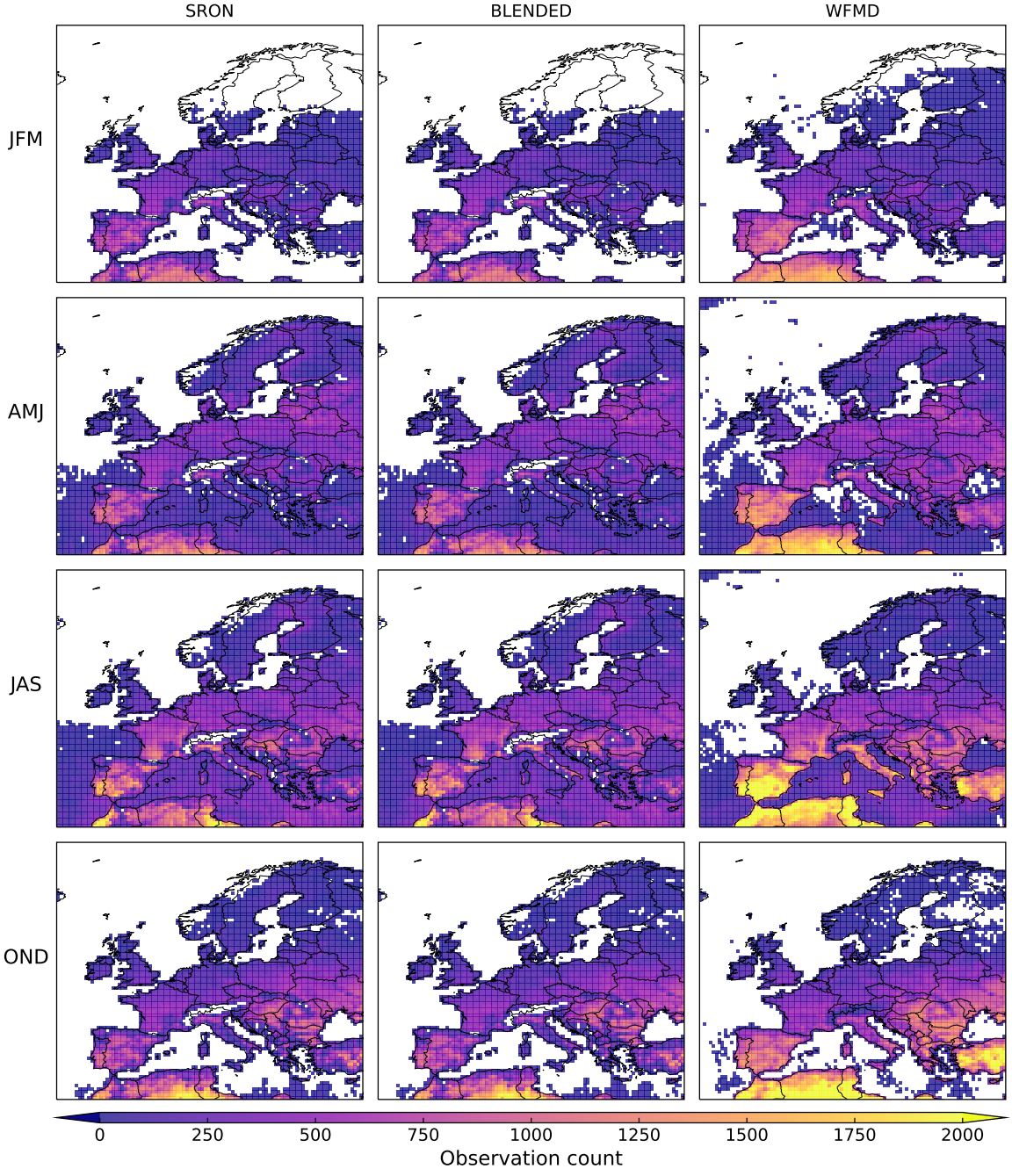
SRON
BLENDED
WFMD
JFM
AMJ
JAS
OND
0
250
500
750
1000
1250
1500
1750
2000
Observation count

(a)

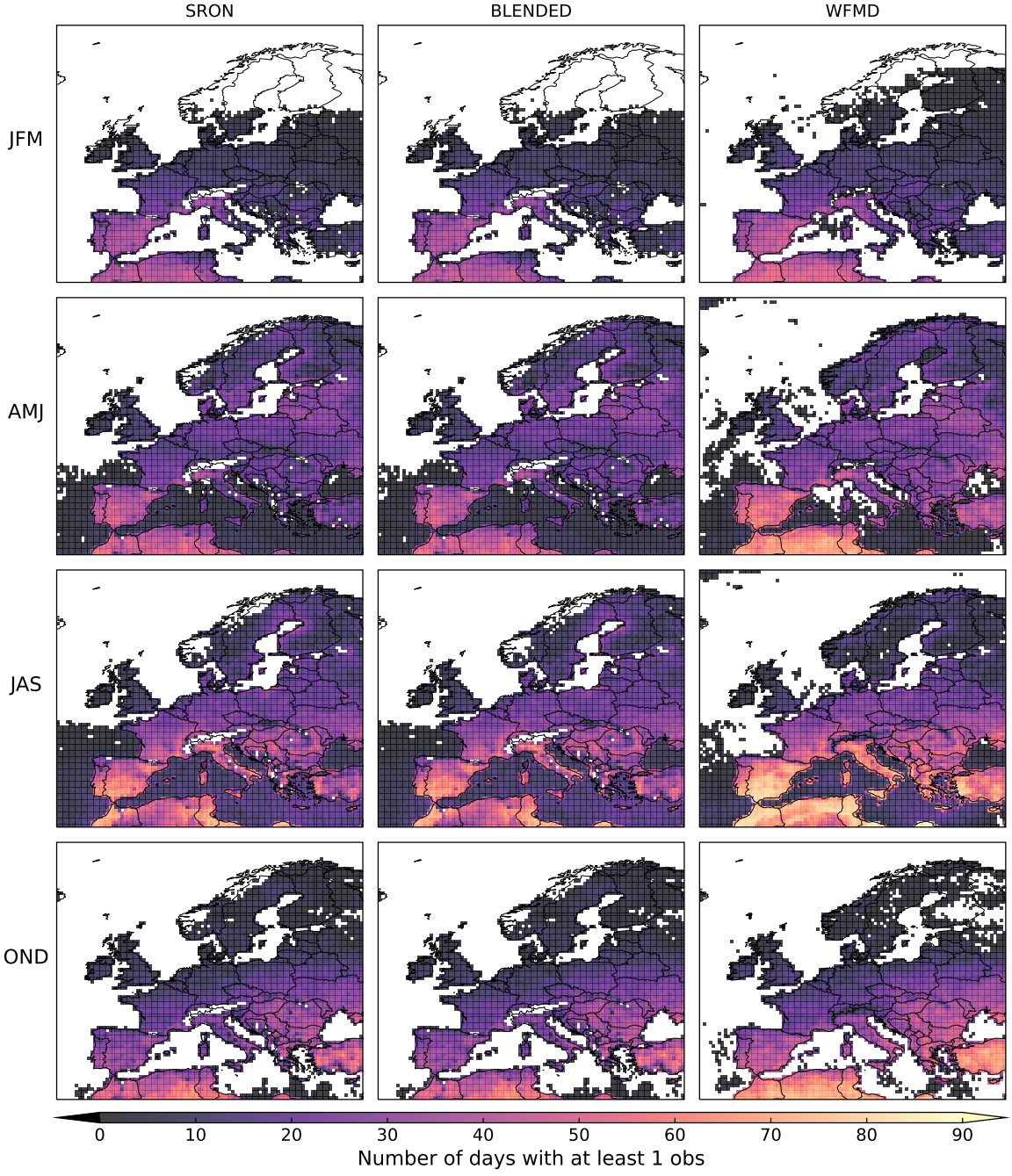

(b)

Figure S1. Seasonal maps of **(a)** the density of observations and **(b)** the number of days with at least one observation, for each CHIMERE 0.5°×0.5° pixel. The three columns correspond to the SRON, BLENDED and WFMD products, while the rows correspond to the seasons.

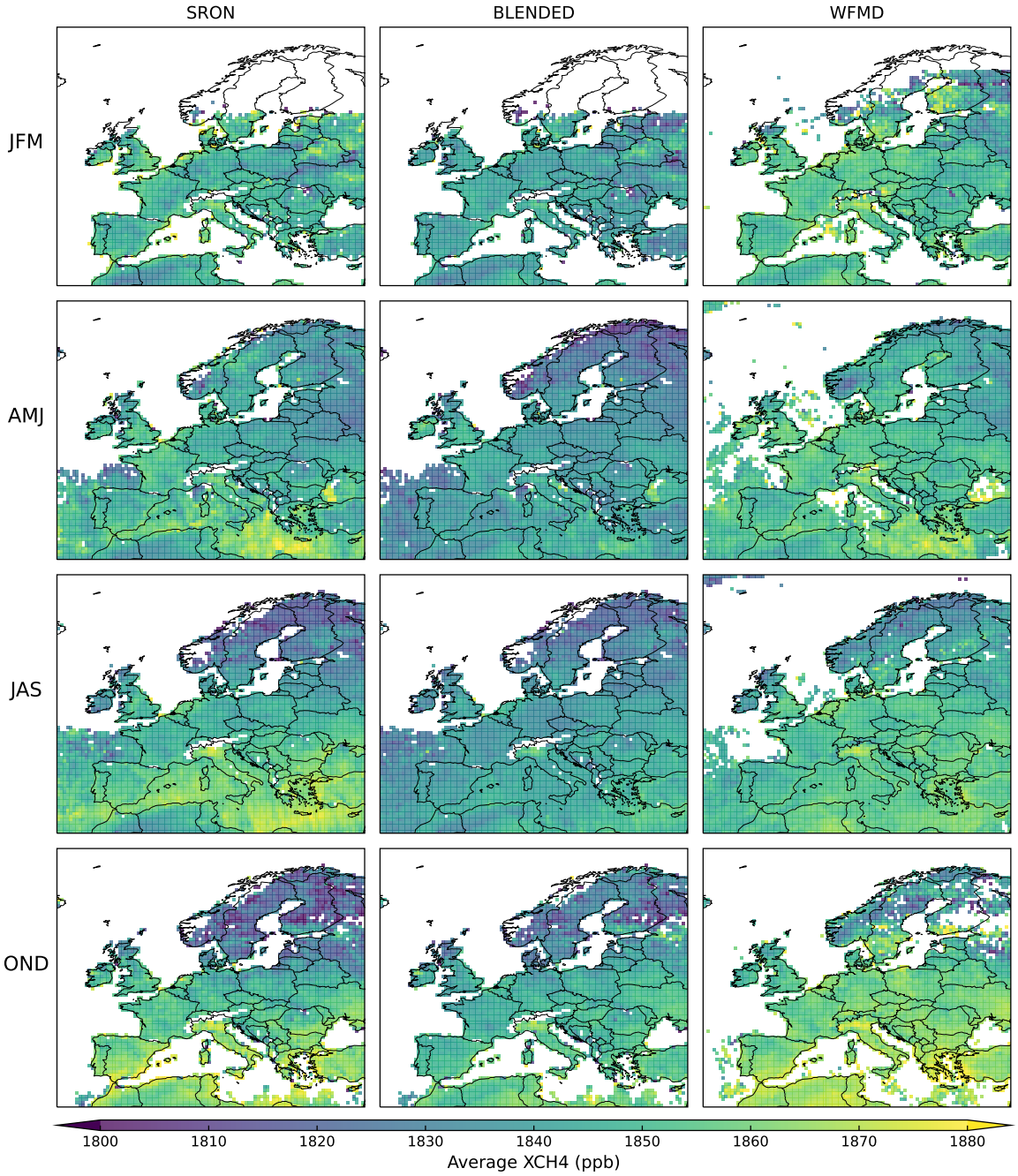

Figure S2. Seasonal average TROPOMI observations (in ppb) for the 3 products.

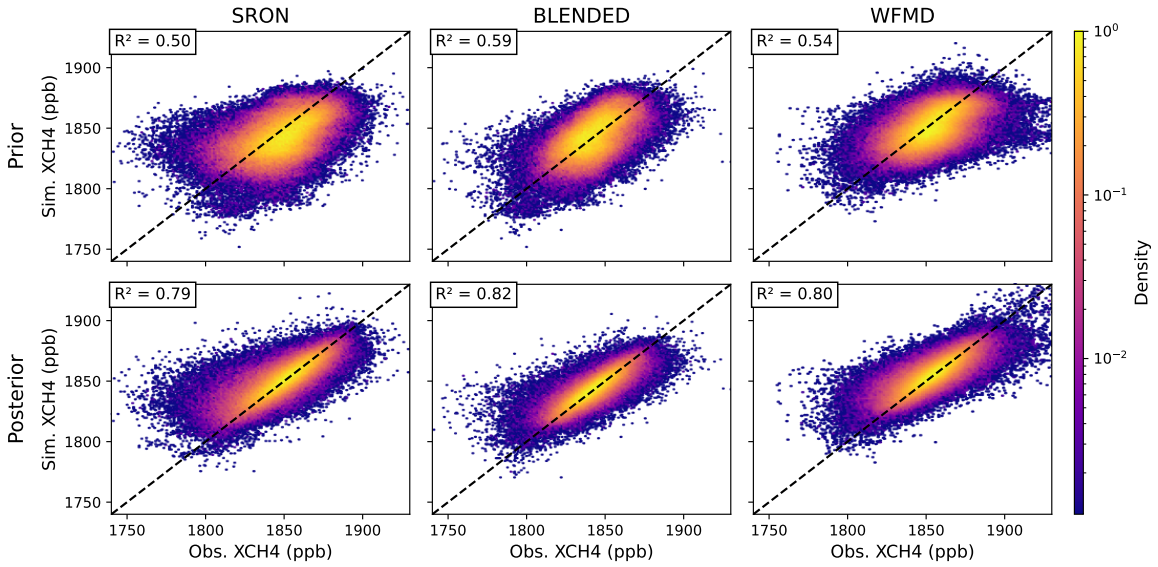

Figure S3. Hexagonal binning plots of the modeled and observed XCH_4 for the TROPOMI inversions, using prior emissions (first row) and posterior emissions (second row). R^2 is the correlation coefficient. The dashed black line is the 1:1 line.

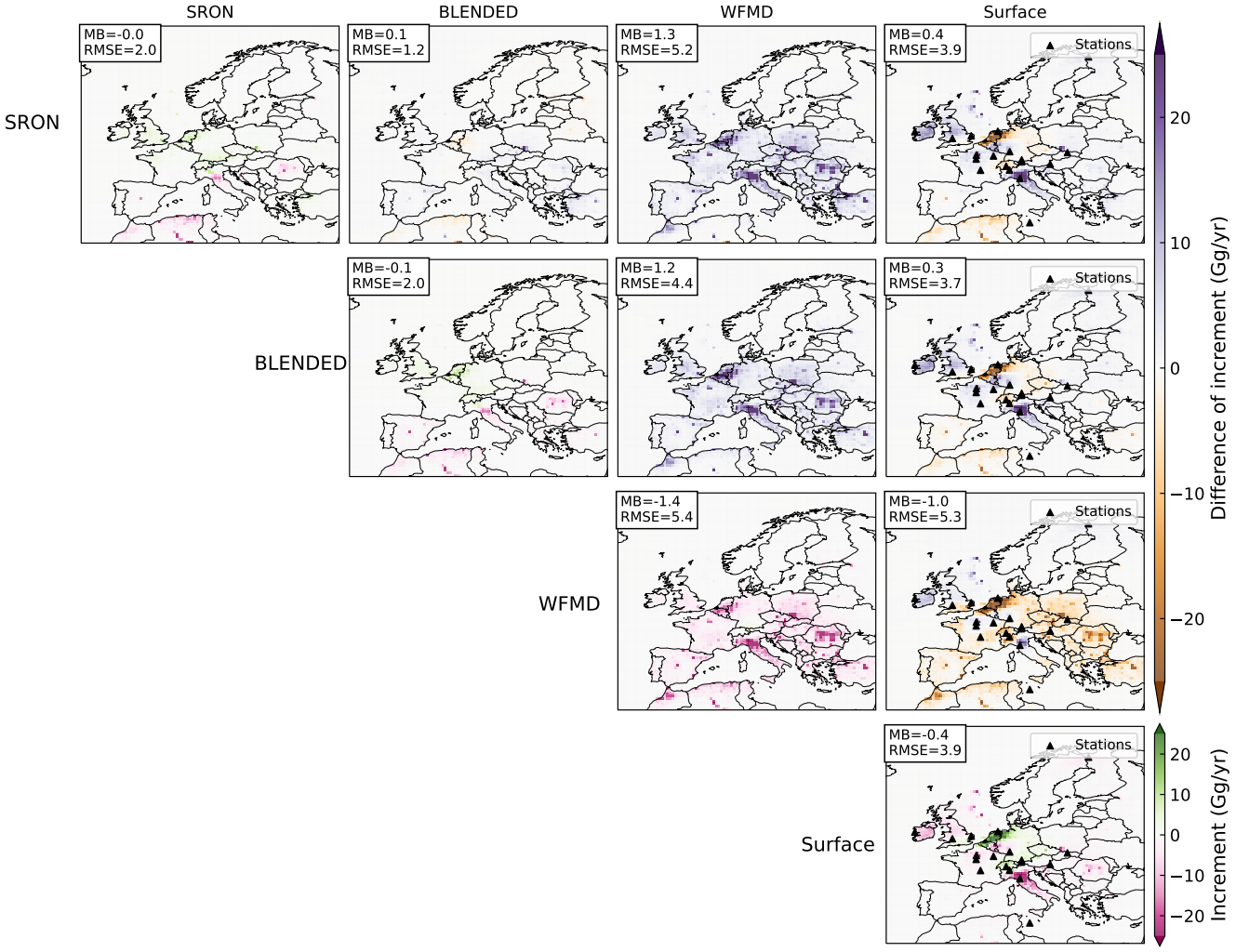

Figure S4. Matrix of the increment maps detailed in Section 3.3. The diagonal maps show the increments as in Figure 10a, while the non-diagonal maps show the difference between the increments derived from the inversions based on the product of the corresponding row and the corresponding column. MB and RMSE are in Gg/yr.

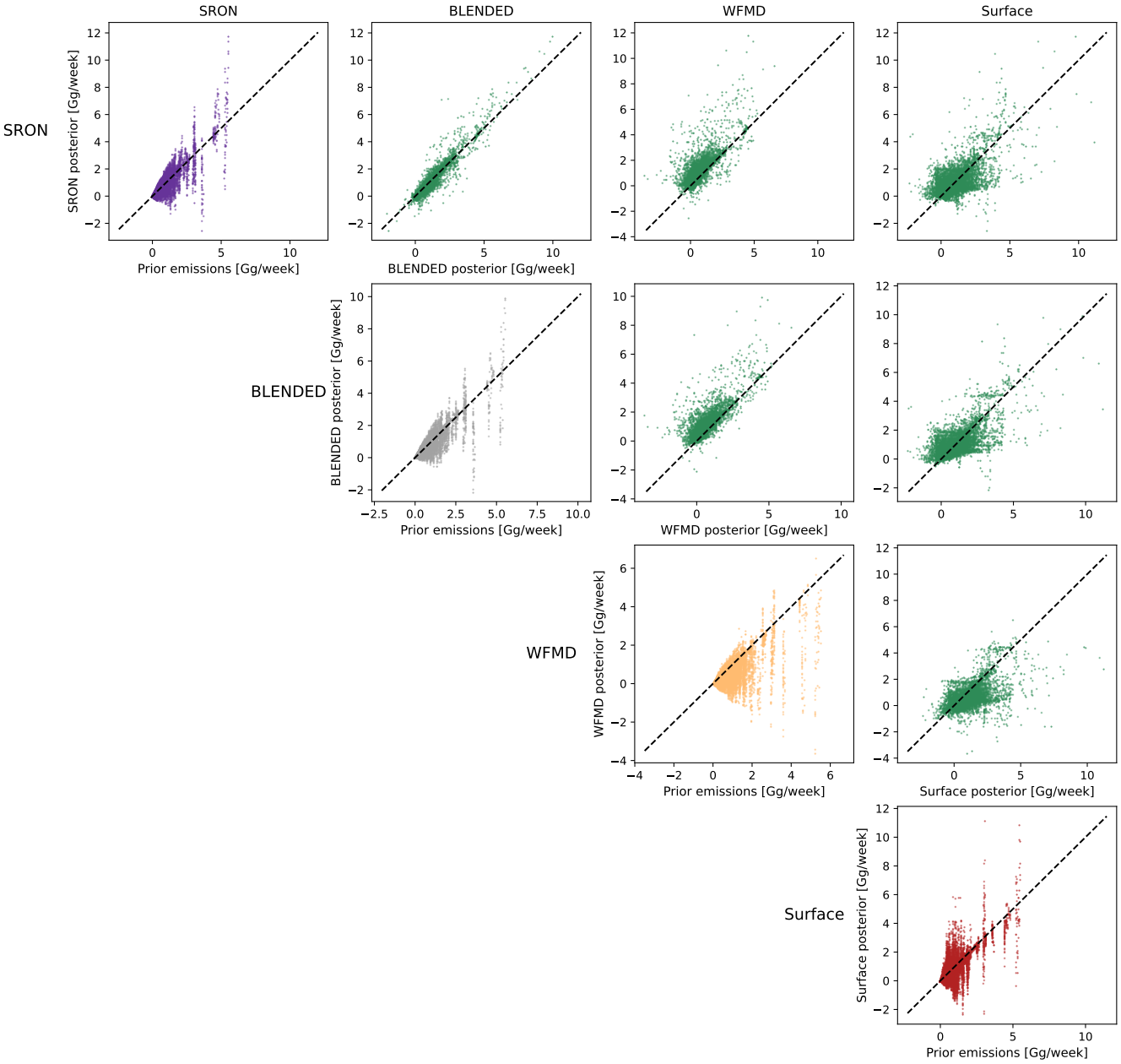

Figure S5. Scatter plots of CH_4 emissions across the four inversions. The diagonal plots show posterior against prior emissions. The non-diagonal plots show a comparison of the posterior emissions. Each scatter point corresponds to a $0.5° \times 0.5°$ pixel and one week, i.e. one element of the control vector. The dashed line is the $x = y$ line.

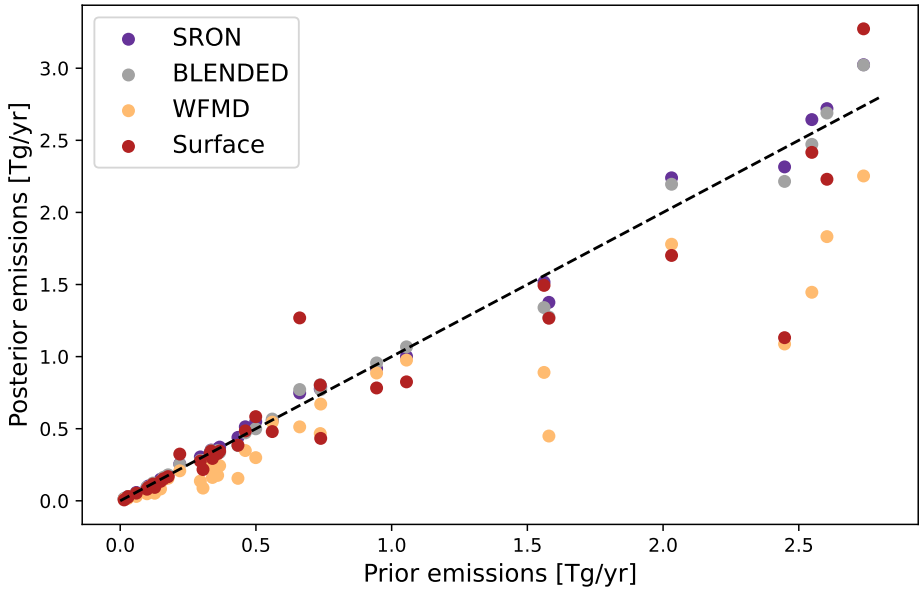

Figure S6. Scatter plot of the yearly and country averaged CH_4 prior and posterior emissions, across the four inversions. Each scatter point corresponds to a country.

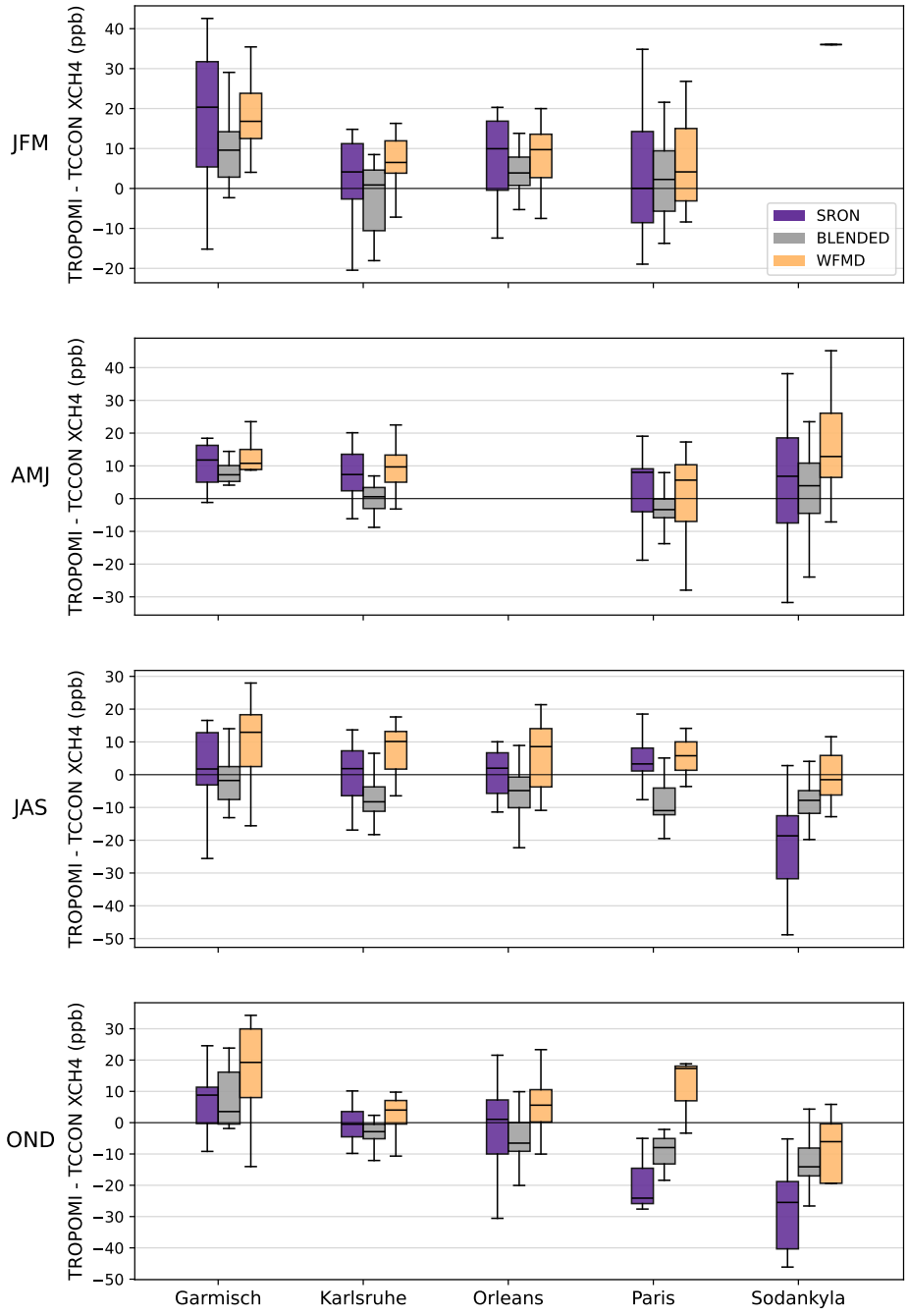

Figure S7. Similar as Figure C1, but for all 4 seasons: median and quartiles of the daily averaged differences between TROPOMI and TCCON XCH4 (ppb) for 5 TCCON stations, per season.

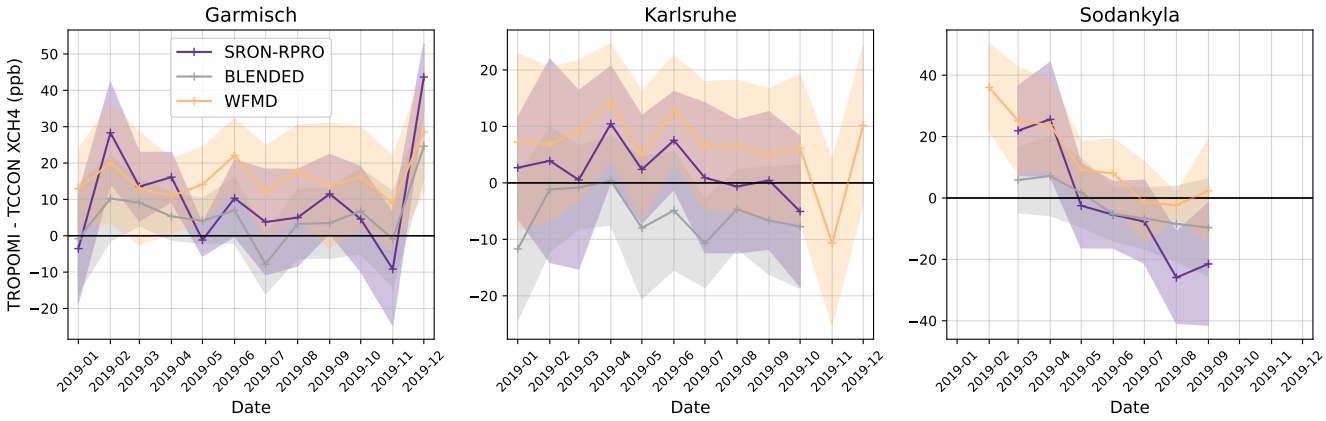

Figure S8. Time series of the monthly averaged differences between TROPOMI and TCCON XCH4 (ppb), for 3 stations. The shaded area shows the standard deviation within each month.